

ANALYSIS OF THE INTERACTION BETWEEN VERTEBRAL LATERAL DEVIATION AND AXIAL ROTATION IN SCOLIOSIS

IAN A. F. STOKES and MACK GARDNER-MORSE

University of Vermont, Department of Orthopaedics and Rehabilitation, Burlington, VT 05405, U.S.A.

Abstract—There is a lack of clear biomechanical analyses to explain the interaction of the lateral and axial deformity of the spine in idiopathic scoliosis. A finite element model which represented an isolated ligamentous spine with realistic elastic properties and idealized geometry was used to analyse this interaction. Three variations of this model were used to investigate two different hypotheses about the etiology of scoliosis and to define the forces required to produce a scoliosis deformity. The first hypothesis is that coupling within a motion segment produces the interaction between lateral deviation and axial rotation. The second hypothesis is that posterior tethering by soft tissues in the growing spine produces the observed interaction. Modeling of both hypotheses failed to produce the clinically observed pattern of interaction.

Therefore, to find which biomechanical forces were required to produce an idealized scoliosis, prescribed displacements were applied to the model. Production of a double curve scoliosis of 10° Cobb angles required lateral forces on the order of 20 N acting 40 mm anterior to the vertebral body centers. There do not appear to be any anatomic structures capable of producing such forces. Therefore, it seems unlikely that scoliosis deformity can be explained in terms of forces acting on the spine, and understanding of its origins may come from examination of other mechanisms such as asymmetric thoracic growth, or asymmetric vertebral development.

INTRODUCTION

An important feature of idiopathic scoliosis deformity is the vertebral axial rotation which accompanies the vertebral lateral deviation. Mechanical interactions within the spine have been implicated in causing vertebral rotation with lateral deviation. This rotation is thought to be significant for initiation and progression of scoliosis. The magnitude of vertebral axial rotation correlates with the lateral deviation of vertebrae from the spinal axis, and the rotation is maximal near the curve apex (Stokes *et al.*, 1987, 1988). The vertebral axial rotation usually rotates the spinous processes towards the concavity of the scoliosis. The cause of this interaction between vertebral deviation and axial rotation is not understood.

The relationship between vertebral lateral deviation and axial rotation in scoliosis has been compared with normal spinal kinematic behavior in lateral bending movements. Lovett (1905) noted that vertebral axial rotation was dependent on whether the spine was flexed or extended during lateral bending movement. Arkin (1950) confirmed this with X-rays. Motion of the whole spine is dependent on the kinematics of the motion segments. It is known that motion segments have 'coupled motion'. Coupling is defined as motion about one axis which is consistently associated with motion about a second axis (White, 1971). White (1971) studied this coupling quantitatively and showed that these kinematic relationships might explain the eventual shape of a deformed spine. Scholten (1986) used a mathematical model to show that the

kinematics of the whole spine also depends on the spinal curvature.

An alternative theory, the 'rotational lordosis', was developed by Somerville (1952). This theory proposes that accelerated anterior growth or constrained posterior growth forces the spine into a combination of lordosis, rotation and lateral deviation. This was demonstrated both in a physical model and in the spines of growing rabbits whose spinous processes were wired together. Dickson and colleagues developed the Somerville theory through animal experiments (Smith and Dickson, 1987), morphologic studies (Deacon *et al.*, 1984; Dickson *et al.*, 1984) and developed a surgical approach based on their observation of hypokyphosis in patients with thoracic scoliosis (Dickson and Archer, 1987). In a related theory it is proposed that scoliosis is caused by soft tissue constraints (a 'tether') interacting with unequal growth of the vertebrae (Roaf, 1966). Jarvis *et al.* (1988) experimented with a posterior tether which they suggested was the mechanism behind the rotational lordosis. They applied a metal rod or wire to excised human and calf spines, and showed in one case of each species that compression of this construct caused both a lateral curvature and some degree of rotation of the spinous processes towards the concave side of the resulting curve.

In this study a finite element model was used to investigate these two different hypotheses about the development of vertebral lateral deviation and axial rotation in scoliosis. The first hypothesis is that coupling within a motion segment produces the interaction between vertebral lateral deviation and axial rotation. The second hypothesis is that posterior tethering by

soft tissues as the spine grows produces the observed interaction. In a third simulation, the finite element model was used to calculate the forces required to deform an initially straight spine into an idealized scoliosis deformity. The purpose of these simulations was to determine which biomechanical factors are important to produce a deformity with both lateral curvature and vertebral axial rotation in an elastic spinal model.

METHODS

The analysis was performed using finite element models of an isolated ligamentous thoracic and lumbar spine. The elastic deformations and forces were calculated by a finite element analysis program (SAP implementation by Algor, Inc., Pittsburg, PA).

The geometry of the model was idealized. In order to investigate the sensitivity of the models to the initial geometry, two different sagittal plane profiles were investigated. In the first, the initial shape was straight in the back view and in the form of a sine wave in the lateral view. The Cobb angle of the complementary lordosis and kyphosis was 40° (Fig. 1). The second geometry represented the realistic shape of the kyphosis and lordosis by using a sixth order polynomial given by Cramer *et al.* (1976). This has a thoracic kyphosis of 38° Cobb and a lumbar lordosis of 20° Cobb. The inflection point between curves is at T11. To provide a means for visualizing the geometry of the model, and to provide attachment points for the

posterior tether, three beam elements representing vertebral processes were attached to the nodal positions corresponding to the center of each vertebral body.

The model was constrained by restricting axial rotation of both end vertebrae, along with the translational constraints shown in Fig. 1 in order to keep the alignment of the head relative to the pelvis as seen *in vivo*.

The models were simplified by having motion segments of equal length. These idealized geometries each defined 17 nodal points representing the centers of the vertebral bodies from T1 to L5. The model used 16 identical stiffness matrices to represent the motion segments which linked the 17 vertebrae. The 6×6 stiffness matrix for thoracic motion segments published by Panjabi *et al.* (1976) gave the relationship between applied forces and corresponding displacements at the loaded node. The assumptions of bilateral symmetry and conservation of energy leave 12 unique nonzero terms in this matrix (Panjabi *et al.*, 1976). The six diagonal terms give the stiffnesses for displacements in the same directions as the applied forces. The six off-diagonal terms describe coupling relationships. The 6×6 matrix was used to create the 12×12 matrix for the two-node motion segment element in these models, as described by Gardner-Morse *et al.* (1990).

Initially, the motion segment matrix was incorporated directly into the model, thereby including all six coupling terms. In further simulations used to establish the importance of the coupling terms, the motion segment element was replaced by a beam element with comparable stiffness properties (Gardner-Morse *et al.*, 1990), referred to here as the 'equivalent' beam element. The stiffness matrix of the beam element matched the diagonal terms of the experimental matrix, but approximated only two of the coupling terms. These were the terms for lateral displacement/rotations and sagittal displacement/rotation. The omitted terms were axial rotation/lateral rotation; axial rotation/lateral displacement; axial displacement/sagittal rotation; and axial displacement/sagittal displacement.

Three different models were studied. The first model is called the 'Coupling Model' and was used to investigate coupling relationships within the ligamentous spine in response to forces and moments that produce lateral curvature. Moments were applied to the ends of the coupling model to produce either single or double curvature deformities. Moments in opposite directions produced a single curve, and moments in the same direction (along with lateral forces to restore equilibrium) produced a double curve (Fig. 2).

The second model is called the 'Tether Model'. A postero-lateral tether consisting of spring elements was added to connect the vertebral processes on the righthand side (Fig. 1). To examine the Somerville (1952) hypothesis, the tether was shortened by applying initial strains to the spring elements, to produce deformed spinal shapes. To simulate the Jarvis *et al.*

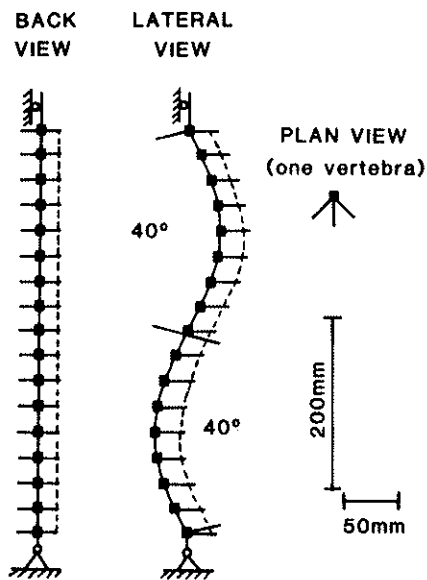


Fig. 1. Back, lateral and plan views of the model of an idealized thoracic and lumbar spine. There are 17 equally spaced vertebral nodes (shown as squares) in the form of a sine wave, with vertebral processes attached to each node. In the tether model, spring elements (shown as dashed lines) linked adjacent postero-lateral processes on the right side.

These springs were omitted from the coupling model.

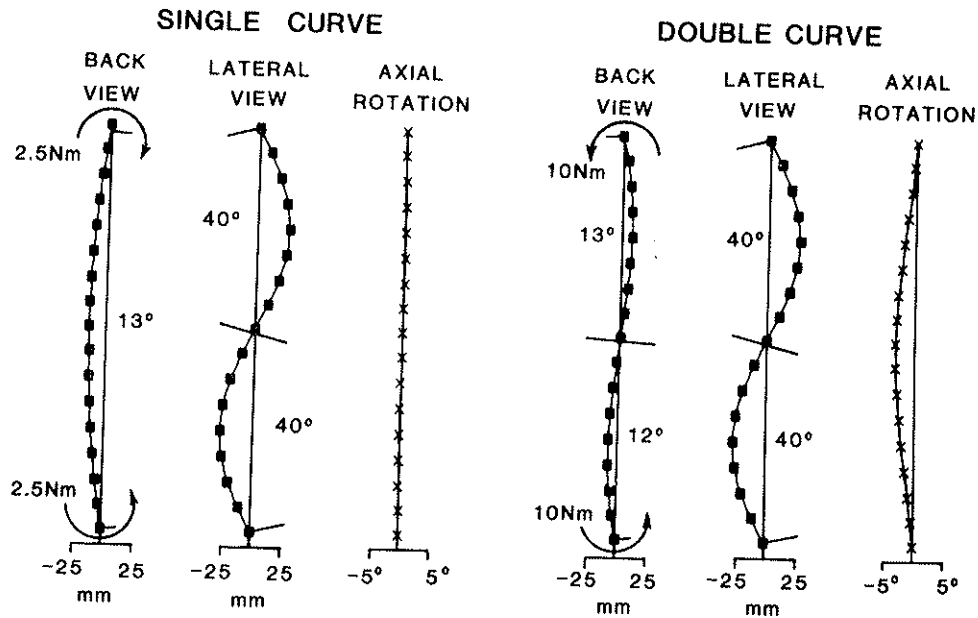


Fig. 2. Outputs of coupling model simulations showing resulting geometry with vertebral position plotted on the vertical axis. Back and lateral views of the vertebrae are shown with square (■) symbols and the vertebral axial rotation with × symbols. (Left) the single curve coupling model; (right) the double curve coupling model. On the horizontal axes positive values signify right vertebra positions, posterior vertebra positions, and clockwise rotations (as seen from above). Neither model produced the clinically observed pattern of spinal deviation and vertebral rotation.

(1988) experiment, compressive forces were applied to this model.

The third model, called the 'Prescribed Displacement Model', applied prescribed lateral deviations and axial rotations to the vertebrae. Two different prescribed deformities were investigated in this model for each of the two sagittal plane geometries. The first frontal plane shape was a full sine wave which had 10° Cobb angles. The second used the geometry of a buckled beam with both ends fixed, and the mid point pinned to give a double curve (Case and Chilver, 1959). The major difference between the frontal plane geometries was in the slopes at the ends. In both cases the axial rotation applied to each vertebra was $0.45^\circ \text{ mm}^{-1}$ of applied lateral deviation as observed clinically by Stokes *et al.* (1988). The finite element model was used to calculate the remaining displacements, and the resulting forces and moments (Weaver and Gere, 1980).

RESULTS

The models were evaluated by how well they matched the clinically observed relationship of vertebral axial rotation and lateral deviation. Vertebral axial rotations were referred to as either clockwise or counterclockwise, as seen from above.

Coupling model

The effects of three variables were investigated: the application of single or double curve moments, repres-

entation of motion segment stiffness, and sagittal plane geometry.

The moments required to produce a double curve were four times greater than those which produced a single curve of the same magnitude (2.5 and 10 Nm respectively, to produce curves of 13° Cobb). Figure 2 shows the deformed shapes in the back view and lateral view of the model, and the accompanying vertebral axial rotations. Vertebral rotation was of a different pattern for single and double curves. In the single curves there was minimal vertebral axial rotation (up to 0.10° for the sine wave sagittal profile) but it was clockwise in the thoracic region and counterclockwise in the lumbar region. In the double curves, the maximum vertebral axial rotation was 3.2° with the sine wave sagittal profile and the rotation was always in the counterclockwise direction.

To examine the effects of removing some of the intersegmental coupling, the models were run again with the intervertebral stiffness matrices replaced by the 'equivalent' beam elements. The results were qualitatively very similar to those from the original coupling model, but the 'equivalent' beams gave somewhat less vertebral axial rotation. Both single curve models produced minimal vertebral axial rotation. The double curve model produced maximum vertebral axial rotation of 2.2° compared with 3.2° . Thus, the presence of coupling terms in the motion segment stiffness had little effect on the behavior of the coupling model.

With the Cramer *et al.* (1976) sagittal plane profile, the vertebral lateral deviation was the same as for the

sine wave geometry, but the axial rotations were different. For the double curve, the maximum vertebral axial rotation moved from the mid point of the model, but remained close to the inflectional point between kyphosis and lordosis. The importance of the sagittal geometry was confirmed when the simulations were repeated with the lordosis and kyphosis removed to give an initially straight spinal shape, and only minimal vertebral axial rotation resulted. Also, when the initial sine wave kyphosis and lordosis of the coupling model were increased from 40 to 72°, the vertebral axial rotation increased by about the same proportion.

Thus, the behavior of the coupling model resulted primarily from the initial sagittal plane geometry, and not from the coupling behavior of the intervertebral joints.

Tether model

Contraction of the postero-lateral tether by 3% produced a single lateral curvature, Cobb angle 14°, deviating away from the tethered side. The tether also reduced the kyphosis by 9° and increased the lordosis by 8°. There was up to 0.9° of vertebral axial rotation in the sine wave model. The vertebral axial rotation was counterclockwise (correct) in the kyphotic region and clockwise (incorrect) in the lordotic part of the spine (Fig. 3). The rotation was different for the two sagittal profiles (the sine wave and the Cramer *et al.* (1976) geometries). The patterns of axial rotation matched the sagittal plane profiles, rather than the pattern of lateral deviation.

A compression force of 250 N applied to the tether model (to simulate the Jarvis *et al.* (1988) experiment) produced deformed shapes similar to those of the contracted tether. Differences were due to the tether being forced into compression in the lordotic region.

Since it was noted that the most realistic pattern of vertebral axial rotation and lateral deviation occurred in the kyphotic thoracic part of this model, a further model run was performed with the tether only in this upper part of the spine. This model produced a single curve with vertebral axial rotation to the correct side. Although the lateral displacement continued below the tether, the axial rotation did not, as shown in Fig. 3. Also, the apex axial rotation was only 0.09° mm⁻¹ of apex lateral deviation.

As in the coupling model, it was found that minimal changes resulted when 'equivalent' beam elements were used instead of the experimental stiffness matrices to represent the motion segments.

The axial rotation was again found to be sensitive to the sagittal plane profile. When the initial kyphosis and lordosis were increased, the axial rotation increased by the same proportion. With both the sine wave and the Cramer *et al.* (1976) initial geometry, the pattern of axial rotation matched the sagittal profile.

Prescribed displacement model

Two variables in the prescribed displacement model were investigated. These were the frontal plane shape produced by the prescribed displacements (sine wave or buckled beam shape) and the initial sagittal plane geometry (sine wave or Cramer *et al.* (1976) geometry).

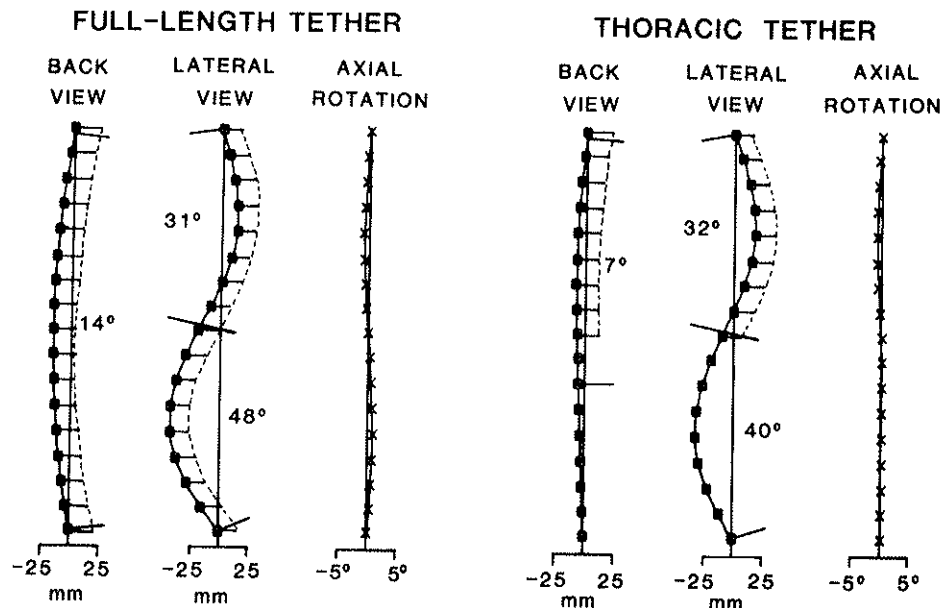


Fig. 3. Output of tether model simulations showing resulting spinal shape with vertebral position plotted on the vertical axis. Back and lateral views of the vertebrae are shown with square (■) symbols and the vertebral axial rotation with × symbols. (Left) the full length postero-lateral tether; (right) postero-lateral tether in the thoracic region only. On the horizontal axes, positive values signify right vertebra positions, posterior vertebra positions, and clockwise rotations (as seen from above). Only the thoracic tether produced vertebral rotation in the correct direction, although of very small magnitude.

The lateral forces and axial moments required to produce a sine wave-shaped scoliosis are shown in Fig. 4. The forces and moments were not symmetric despite the symmetric initial and final geometries. The lateral forces were of the order of 20 N and the axial moments were of the order of 1 Nm to make a sine wave scoliosis of 10° Cobb. The force and moment on each vertebra could be replaced by a single offset force. These offsets were found to be approximately 40 mm anterior to the vertebral centers.

Similar patterns of lateral forces and axial moments were required to create a scoliosis of the same lateral deviation but with a buckled beam shape instead of a sine wave. However, the lateral forces were $2.5 \times$ as great and the axial moments were $1.4 \times$ as great. In contrast, the shape of the sagittal profile had minimal effect on the forces and moments.

DISCUSSION

This study addresses two different hypotheses about the development of vertebral lateral deviation and axial rotation in scoliosis. Simulations were used to examine the hypotheses that (1) normal inherent coupling within a motion segment and (2) posterior tethering by soft tissues produce this interaction. A third simulation calculated the forces required to deform an initially straight spine into an idealized scoliosis deformity.

There were a number of assumptions in these models. They assumed linear elastic behavior of the motion segments, normal growth, and the head was

made to remain aligned with the pelvis by simple end constraints. Other anatomical structures (muscle actions and the rib cage) were omitted. The assumption of elastic behavior implies that removal of the forces would result in reversal of the deformity. While time-dependent behavior may alter the magnitudes of residual forces and deformations, this relaxation would not change the resulting patterns. Therefore, this model can indicate the initial direction and pattern of a deformity resulting from the application of forces simulated here.

The models do not include other long-term effects such as growth, remodeling of bone, and modulation of growth (Karaharju, 1967; Roaf, 1963, 1966). Disturbed growth has been implicated in producing vertebral abnormalities in scoliosis (Deane and Duthie, 1973; Roaf, 1963, 1960). However, Arkin (1949) recognized that vertebral wedging might be primary or secondary. How the resulting vertebral wedging might produce both spinal lateral deviation and vertebral rotation is not clear.

The rib cage, muscles and other structures were omitted from these models in order to examine the specific role of the spine. End constraints were used to model the complex neuromuscular functions which maintain the head in alignment with the pelvis. Haderspeck and Schultz (1981), in a model of scoliosis progression, simulated 68 muscle slips which were recruited in order to achieve the same objective. The external constraints (boundary conditions) are a simplification in that they do not apply compressive loads to the spine. However, compressive loads tended to

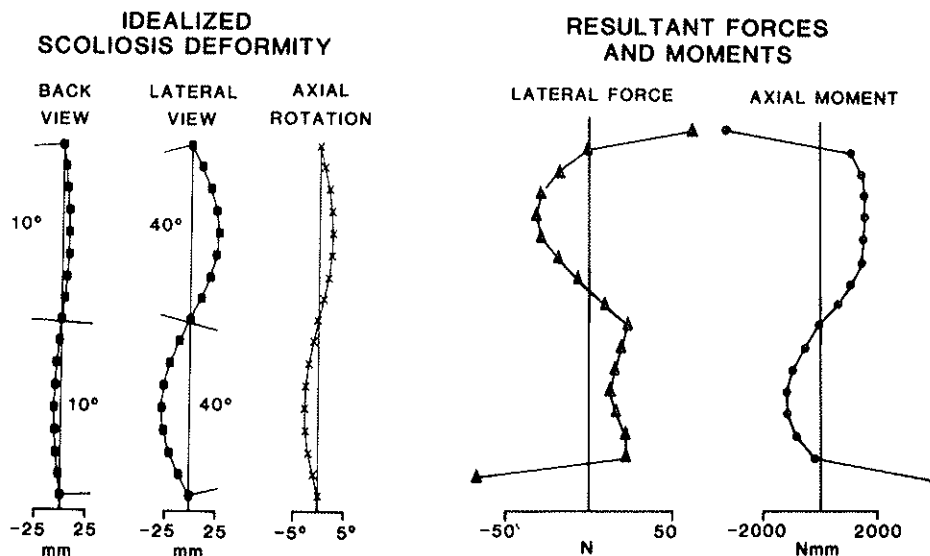


Fig. 4. The prescribed displacement model which produced an idealized scoliosis. Vertebral positions are plotted on the vertical axis. (Left) back and lateral views of the vertebrae are shown with square (■) symbols and the vertebral axial rotation with × symbols. On the horizontal axes positive values signify right vertebra positions, posterior vertebra positions, and clockwise rotations (as seen from above). (Right) lateral forces (▲) and axial moments (●) acting at the center of each vertebral body. Positive forces act to the left and positive moments are clockwise from above. The required forces and moments are equivalent to a force applied anterior to the spine.

increase the sagittal curvature of the spine. Overall, the boundary condition approach seemed a reasonable simplification in these models. In the tether model, the tether only crossed single motion segments. It is possible that posterior muscles and ligaments which span multiple segments of the spine could form more complex tethers.

In a scoliosis the direction of the intersegmental axial rotation reverses at the apex of the curve while the direction of the intersegmental lateral bending does not. This implies that coupling of these two rotations in motion segments would have to reverse at the curve apex. The available data on variation of coupling terms by level of the thoracic spine indicate that this is not the case (Panjabi *et al.*, 1976). Scholten and Veldhuizen (1985) studied the varying angle of the facet joints and demonstrated that more coupling between lateral bending and axial rotation should occur in the thoracic spine than in the lumbar spine. Schultz *et al.* (1979) found that coupling of axial rotation and lateral rotation was seldom inherent in the lumbar spine. In contradiction, Panjabi *et al.* (1989) measured the response of complete lumbar spine specimens to application of axial and lateral bending torques, and reported coupling behavior with differences at different anatomic levels. A possible interpretation of these findings is that they result from the geometric effects of the initial curvature of the lumbar spine specimens, rather than intrinsic coupling within the motion segments. Therefore, it seems reasonable to assume that motion segment coupling does not vary by level throughout the thoracic and lumbar spine of our models.

In our simulations with the coupling model, the inherent coupling within the motion segments was of little importance relative to the initial sagittal plane geometry. Altering this shape substantially altered the results of the simulations. The coupling model demonstrates that the normal inherent coupling found within motion segments does not account for the axial rotation that accompanies the lateral deviation in scoliosis. Veldhuizen and Scholten (1987) similarly concluded from qualitative arguments and observations of patients that the vertebral axial rotation in idiopathic scoliosis could not be explained by spinal kinematics alone.

In the simulations with the tether model, contraction of the tether was used to produce the deformed spinal shape. The resulting spinal shape was equivalent to that produced by elongation (growth) of vertebrae with a passive tether. Simple compressive forces (gravity or muscular forces), or forces in a symmetric tether only increased the sagittal curvature rather than producing a lateral curvature. With the tether only in the thoracic region, an approximately correct pattern of rotation resulted, but the magnitude of the rotation was small. Thus the tether may help explain the development of scoliosis in a kyphotic part of the spine, but leaves double and lumbar scoliosis curves unexplained.

The elastic buckling theory has been used to explain the progression of scoliosis in the rotational lordosis theory (Cruickshank *et al.*, 1989) and in functional scoliosis (Lindbeck, 1985). This is not realistic for idiopathic scoliosis since progression does not occur suddenly, but develops slowly over time. Also, in a three-dimensional analysis of critical load, Scholten (1986) showed that the buckling modes would be in the sagittal, not frontal plane of the spine.

The behavior of the tether model was also very dependent on the initial sagittal plane curvature of the spine. Our simulations of the Jarvis *et al.* (1988) experiment with a human and a calf spine suggest that the small reported rotations were probably also due to the initial shape of the specimens. However, neither the initial nor final curvatures of these spines were reported.

In the prescribed displacement model, the forces necessary to produce a scoliosis were not symmetric in the kyphotic and lordotic regions of the spine despite symmetric geometry and were found to lie anterior to the spine. This raises a question of what anatomic structure might be able to produce such forces. *In vivo*, there are passive forces (tension in soft tissues, etc.), active forces (from muscles), and external forces (gravity, etc.), but it is not clear how these forces would generate horizontal components acting anterior to the spine.

These simulations show that the interaction of vertebral lateral deviation and axial rotation in scoliosis is not explained by the normal inherent coupling within spinal motion segments, nor by tethering of vertebral processes. The prescribed displacement model shows that forces required to produce a scoliosis would act anterior to the spine; however, it is not clear which anatomic structures could produce such forces. Therefore, it seems unlikely that scoliosis deformity can be explained in terms of forces acting on the spine, and understanding of its origins may come from examination of other mechanisms such as asymmetric thoracic growth, or asymmetric vertebral development.

Acknowledgements—Supported by NIH grants R01 AR 38507 and R01 AR 40093. Dr Jeffrey P. Laible assisted in the original formulation of the models.

REFERENCES

- Arkin, A. M. (1949) The mechanism of the structural changes in scoliosis. *J. Bone Jt Surg.* **31A**, 519–528.
- Arkin, A. M. (1950) The mechanism of rotation in combination with lateral deviation in the normal spine. *J. Bone Jt Surg.* **32A**, 180–188.
- Case, J. and Chilver, A. H. (1959) *Strength of Materials*, pp. 350–352. Edward Arnold, London.
- Cramer, H. J., Liu, Y. K. and von Rosenberg, D. U. (1976) A distributed parameter model of the inertially loaded human spine. *J. Biomechanics* **9**, 115–130.
- Cruickshank, J. L., Koike, M. and Dickson, R. A. (1989) Curve patterns in idiopathic scoliosis: a clinical and radiographic study. *J. Bone Jt Surg.* **71B**, 259–263.

- Deacon, P., Flood, B. M. and Dickson, R. A. (1984) Idiopathic scoliosis in three dimensions. A radiographic and morphometric analysis. *J. Bone Jt Surg.* **66B**, 509-512.
- Deane, G. and Duthie, R. B. (1973) A new projectional look at articulated scoliotic spines. *Acta orthop. scand.* **44**, 351-365.
- Dickson, R. A. and Archer, I. A. (1987) Surgical treatment of late-onset idiopathic thoracic scoliosis. The Leeds procedure. *J. Bone Jt Surg.* **69B**, 709-714.
- Dickson, R. A., Lawton, J. O., Archer, I. A. and Butt, W. P. (1984) The pathogenesis of idiopathic scoliosis. Biplanar spinal asymmetry. *J. Bone Jt Surg.* **66B**, 8-15.
- Gardner-Morse, M. G., Laible, J. P. and Stokes, I. A. F. (1990) Incorporation of spinal flexibility measurements into finite element analysis. *J. biomech. Engng* **112**, 481-483.
- Haderspeck, K. and Schultz, A. (1981) Progression of idiopathic scoliosis. An analysis of muscle actions and body weight influences. *Spine* **6**, 447-455.
- Jarvis, J. G., Ashman, R. B., Johnston, C. E. and Herring, J. A. (1988) The posterior tether in scoliosis. *Clin. Orthop.* **227**, 126-134.
- Karaharju, E. O. (1967) Deformation of vertebrae in experimental scoliosis. The course of bone adaptation and modelling in scoliosis with reference to the normal growth of the vertebra. *Acta orthop. scand. Suppl.* **105**, 9-87.
- Lindbeck, L. (1985) Analysis of functional scoliosis by means of an anisotropic beam model of the human spine. *J. biomech. Engng* **107**, 281-285.
- Lovett, R. W. (1905) The mechanism of the normal spine and its relation to scoliosis. *Bos. med. surg. J.* **153**, 349-358.
- Panjabi, M. M., Brand, R. A. and White, A. A. (1976) Three-dimensional flexibility and stiffness properties of the human thoracic spine. *J. Biomechanics* **9**, 185-192.
- Panjabi, M., Yamamoto, I., Oxland, T. and Crisco, J. (1989) How does posture affect coupling in the lumbar spine? *Spine* **14**, 1002-1011.
- Roaf, R. (1960) Vertebral growth and its mechanical control. *J. Bone Jt Surg.* **42B**, 40-59.
- Roaf, R. (1963) The treatment of progressive scoliosis by unilateral growth-arrest. *J. Bone Jt Surg.* **45B**, 637-651.
- Roaf, R. (1966) The basic anatomy of scoliosis. *J. Bone Jt Surg.* **48B**, 786-792.
- Scholten, P. J. M. (1986) Idiopathic scoliosis. Some fundamental aspects of the mechanical behaviour of the human spine. Ph.D. thesis, Free University of Amsterdam, pp. 72-103. Free University Press, Amsterdam.
- Scholten, P. J. M. and Veldhuizen, A. G. (1985) The influence of spine geometry on the coupling between lateral bending and axial rotation. *Engng Med.* **14**, 167-171.
- Schultz, A. B., Warwick, D. N., Berkson M. H. and Nachemson, A. L. (1979) Mechanical properties of human lumbar spine motion segments—Part I: responses in flexion, extension, lateral bending, and torsion. *J. biomech. Engng* **101**, 46-52.
- Smith, R. M. and Dickson, R. A. (1987) Experimental structural scoliosis. *J. Bone Jt Surg.* **69B**, 576-581.
- Somerville, E. W. (1952) Rotational lordosis: the development of the single curve. *J. Bone Jt Surg.* **34B**, 421-427.
- Stokes, I. A. F., Armstrong, J. G. and Moreland, M. S. (1988) Spinal deformity and back surface asymmetry in idiopathic scoliosis. *J. Orthop. Res.* **6**, 129-137.
- Stokes, I. A. F., Bigalow, L. C. and Moreland, M. S. (1987) Three-dimensional spinal curvature in idiopathic scoliosis. *J. Orthop. Res.* **5**, 102-113.
- Veldhuizen, A. G. and Scholten, P. J. M. (1987) Kinematics of the scoliotic spine as related to the normal spine. *Spine* **12**, 852-858.
- Weaver, W. Jr and Gere, J. M. (1980) *Matrix Analysis of Framed Structures* (2nd edn), pp. 152-164. Van Nostrand Reinhold, New York.
- White, A. A. (1971) Kinematics of the normal spine as related to scoliosis. *J. Biomechanics* **4**, 405-411.